Implementation of predicting elastic internal multiples based on inverse scattering series: synthetic results

Jian Sun* and Kris Innanen*

ABSTRACT

Prediction and removal internal multiples is an increasingly high priority task in seismic data processing, due to the increased sensitivity with which primary amplitudes in quantitative interpretation are now analyzed, however, remains to be a big challenge. The more geological model we build approach to real, the more precise the prediction algorithm can be achieved. In a companion paper (Sun and Innanen, 2016d), we proposed a theoretical framework of elastic internal multiples prediction using inverse scattering series, which works for an elastic isotropic medium. In this paper, we investigate how to prepare the input, and concentrate on how to implement the elastic internal multiples prediction algorithm, using the seismic data generated from an elastic isotropic synthetic model. The analysis of the estimated result is also being examined.

INTRODUCTION

The requirement of increasing sensitivity in primary amplitude quantitative interpretation is highlight as the mining environment becomes to be more complex, which enhances the role and significance of multiple prediction and removal. However, one might speaks the importance of accurate and robust prediction of multiples may now be on the verge of an even greater upward jump, as full waveform inversion puts forward. However, having detailed information of what event type occurs in the data at specified time will be incentive and critical technology, no matter how full waveform processing becomes in the future, because the residual changes could depend critically on the nature of event (Sun and Innanen, 2016a).

Former research indicate that multiple attenuation is high correlated to its classified type. Take into account the influence of free-surface, multiples can be identified as two major classes, surface-related multiple and interbed multiple. Due to its periodic characteristic in τ - p domain, surface-related multiples can be eliminated in a comfortable manner and many innovative technologies have been developed in different domains, such as predictive deconvolution (Taner, 1980), inverse approach using feedback model (Verschuur, 1991), embedding technique (Liu et al., 2000), inverse data processing (Berkhout and Verschuur, 2005; Berkhout, 2006; Ma et al., 2009). However, the attenuation of the other classical multiple, internal multiple, still remains to be a big challenge, especially on land data, even though much considerable progresses have been made recently.

Kelamis et al. (2002a,b) introduced a boundary-related/layer-related approach to remove internal multiples in the post-stack data (CMP domain). Berkhout and Verschuur (2005) extended the inverse data processing to attenuate internal multiples by considering them as the suppositional surface-related multiples through the boundary-related/layer-

---

*University of Calgary, CREWES Project

related approach in common-focus-point (CFP) domain. The same algorithm was applied by Luo et al. (2007) through re-datuming the top of the multiple generators and transforming internal multiples to be 'surface-related'. The common ground of those algorithms is that, as it were, extensive knowledge of subsurface is required;thus if the possibility exists that multiple removal will have to take place with incomplete knowledge of the velocity structure and generators, the ISS approach will be optimal.

By analysing the philosophy of forward scattering series, Araujo et al. (1994) and Weglein et al. (1997, 2003) demonstrated that all possible internal multiples can be reconstructed, in an automatic way, as the combination of those sub-events satisfying a certain criterion, and the processing can be achieved by implementing the inverse scattering series in an appropriate manner. Many incentive research and discussions of inverse scattering series on internal multiple attenuation have been made depending on the variant purposes, (1) correcting predicted amplitude of internal multiples (Zou and Weglein, 2015), and (2) refining the algorithm for certain high priority acquisition styles and environments (Hernandez and Innanen, 2014; Pan et al., 2014; Pan and Innanen, 2015; Pan, 2015; Innanen, 2016b,a; Sun and Innanen, 2014, 2015, 2016a,b).

However, all those research and discussions were on account of one assumption, earth is acoustic, which is unrealistic. As we know, the more realistic the geological model we build is, the more accurate the prediction algorithm becomes to be. Based on the previous work discussed by Matson (1997), a companion paper (Sun and Innanen, 2016d) presented how to derive the elastic internal multiple prediction algorithm using inverse scattering series from multi-component seismic data. Even earth is not an elastic isotropic medium, elastic internal multiple prediction could still be a pioneer to the internal multiple prediction on land data. In this paper, we focus on the preparation and implementation of internal multiples prediction in an elastic isotropic medium.

METHODOLOGY

As many previous works on acoustic internal multiples prediction using inverse scattering series, elastic internal multiples can also be rebuilt with perturbations and a background considered as an elastic isotropic homogeneous medium. The leading-order prediction algorithm was first proposed by Matson (1997), and then was consummated by Sun and Innanen (2016d). For all 1st-order internal multiples attenuation, the 3D methodology can be described as,

$$
\begin{aligned}
b_{3ij}&(k_{ix_g}, k_{iy_g}, k_{jx_s}, k_{jy_s}, \omega) \\
&= -\frac{1}{(2\pi)^4} \iiiint_{-\infty}^{+\infty} \mathrm{d}k_{kx_1} \mathrm{d}k_{ky_1} \mathrm{d}k_{lx_2} \mathrm{d}k_{ly_2} e^{\mathrm{i}\nu_{k1}(z_s-z_g)} e^{-\mathrm{i}\nu_{l2}(z_s-z_g)} \\
&\quad \times \int_{-\infty}^{+\infty} \mathrm{d}z_1 e^{\mathrm{i}(\nu_{k1}+\nu_{ig})z_1} b_{1ik}(k_{ix_g}, k_{iy_g}, k_{kx_1}, k_{ky_1}, z_1) \\
&\quad \times \int_{-\infty}^{z_1-\epsilon} \mathrm{d}z_2 e^{-\mathrm{i}(\nu_{l2}+\nu_{k1})z_2} b_{1kl}(k_{kx_1}, k_{ky_1}, k_{lx_2}, k_{ly_2}, z_2) \\
&\quad \times \int_{z_2+\epsilon}^{+\infty} \mathrm{d}z_3 e^{\mathrm{i}(\nu_{js}+\nu_{l2})z_2} b_{1lj}(k_{lx_2}, k_{ly_2}, k_{jx_s}, k_{jy_s}, z_3)
\end{aligned}
\tag{1}
$$

with,

$$\nu_{IM} = \sqrt{\frac{\omega^2}{c_{I0}^2} - k_{Ix_M}^2 - k_{Iy_M}^2}$$ (2)

where, z is the pseudo-depth (depth in the reference medium), and z_1, z_2, z_3 satisfy the lower-higher-lower relationship, i.e., $z_1 > z_2$ and $z_2 < z_3$. k_{Ix_M} and k_{Iy_M} are x and y components of wavenumber, ν_{IM} is the vertical component of wavenumber. The subscript $M \in \{g, s, 1, 2\}$ means the source or receiver side for a specified ray-path, i.e., k_{Ix_M} is the x component of wavenumber corresponding to location (x_M, y_M, z_M). c_{I0} is the velocity depending on the wave mode I, and $I = (i, j, k, l) \in \{P, SH, SV\}$.
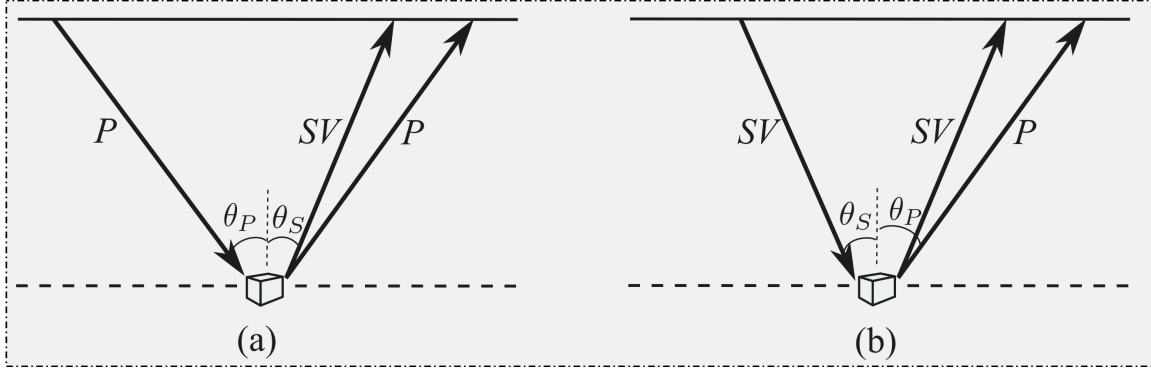

FIG. 1. In 1.5D cases, wave propagation in perturbation mode. (a) P-wave source only, (b) S-wave source only.

Consider a line survey (2D), and assume the earth is layered (Figure. 1), Snell's law can be described as,

$$\frac{\sin \theta_P}{v_P} = \frac{\sin \theta_S}{v_S} = p$$ (3)

where, v_P, v_S represent P- and S-wave velocities, p is the ray-parameter.

Eq. 3 denotes that, for layered cases, we have, $k_{x_s}^P = k_{x_g}^P = k_{x_g}^{SV}$ with P-wave source only, and $k_{x_s}^{SV} = k_{x_g}^{SV} = k_{x_g}^P$ with S-wave source only. Here, to avoid confusion, we use superscripts to denote wave mode type. Therefore, assume $z_s = z_g$, the prediction algorithm for a layered case can be simplified as,

$$b_3^{ij}(k_g^i, \omega) = -\int_{-\infty}^{+\infty} dz_1 e^{i(\nu^m + \nu^i)z_1} b_1^{im}(k_g^i, z_1) \int_{-\infty}^{z_1 - \epsilon} dz_2 e^{-i(\nu^n + \nu^m)z_2} b_1^{mn}(k_g^m, z_2)$$
$$\times \int_{z_2 + \epsilon}^{+\infty} dz_3 e^{i(\nu^j + \nu^n)z_3} b_1^{nj}(k_g^n, z_3)$$ (4)

with,

$$\nu^X = \sqrt{\frac{\omega^2}{(c_0^X)^2} - (k_g^X)^2}$$ (5)

where, ν^X is the vertical wavenumber depending on the wave mode determined by the superscript $X \in \{P, SV\}$, k_g^X is the horizontal wavenumber for P- or S-wave. z is the pseudo-depth meets the same lower-higher-lower relationship as noted above, c_0^X is the

background P- or S- wave velocity. b_1 is the weighted decomposed seismic data, which can be calculated by $b_1^{ij}(k_g^i, \omega) = \mathrm{i}2\nu^j D^{ij}(k_g^i, \omega)$, $\{i, j\} \in \{P, SV\}$. Here, j denotes the source side, and i represents the geophone side.

To further understand the philosophy of prediction algorithm in Eq. 4, assume the source involves P-wave only, i.e, $j = P$ and $i = P$ or S (In following context, S represent SV-wave). Therefore, internal multiples in $P \rightarrow P$ mode and in $P \rightarrow S$ mode can be predicted by the combination of the weighted decomposed data using P-source only, delineated as,

$$b_3^{\acute{P}\grave{P}} = \Theta_1(b_1^{\acute{P}\grave{P}})\Theta_2(b_1^{\acute{P}\grave{P}})\Theta_3(b_1^{\acute{P}\grave{P}}) + \Theta_1(b_1^{\acute{P}\grave{S}})\Theta_2(b_1^{\acute{S}\grave{P}})\Theta_3(b_1^{\acute{P}\grave{P}}) + \Theta_1(b_1^{\acute{P}\grave{P}})\Theta_2(b_1^{\acute{P}\grave{S}})\Theta_3(b_1^{\acute{P}\grave{P}})$$
(6a)

$$b_3^{\acute{S}\grave{P}} = \Theta_1(b_1^{\acute{S}\grave{P}})\Theta_2(b_1^{\acute{P}\grave{P}})\Theta_3(b_1^{\acute{P}\grave{P}}) + \Theta_1(b_1^{\acute{S}\grave{P}})\Theta_2(b_1^{\acute{P}\grave{S}})\Theta_3(b_1^{\acute{S}\grave{P}})$$
(6b)

Here, Θ_X denotes the Xth integral described in Eq. 4, $\grave{P}$ indicates the incident P-wave, $\acute{P}$ represents the received P-wave.

Eq. 6 shows that, in 1.5D case, all possible internal multiples occurred in a single shot gather using non-mixed source, no matter in P-wave model or in S-wave mode, can be predicted by integrating its weighted decomposed components in a certain way. In the upcoming section, to examine the prediction algorithm, Eq. 4 is performed, as the combination shown in Eq. 6 for variant wave modes, on a three-layer elastic isotropic model.

IMPLEMENTATION OF ELASTIC ISS-IMS PREDICTION

Input preparation, implementation domain and search parameter selection are highly correlated and are also key elements for internal multiples prediction (Sun and Innanen, 2016c). However, to concentrate the aim of this paper and to examine the adaptability of this algorithm in the sense of implementation domain, the prediction of internal multiple is performed in plane wave ($\tau - p$) domain, with a constant ϵ for search parameter. In following context, two objectives we focus on are, how to prepare the input data, and how to configure the limits of integral for implementing the prediction algorithm.

A three-layer elastic model is built to create synthetic dataset that prediction will be performed on. The geological model and model parameters are shown in Figure 2, from top to bottom, P-wave velocities are $[2000, 3500, 2500]m/s$, S-wave velocities are $[1200, 2000, 1300]m/s$, and densities are $[1.5, 2.25, 1.6]g/cm^3$. A single shot gather is generated using finite difference in $sofi2D$. And the radial and vertical components are delineated separately in Figure 3. Note that, the polarity is reversed in radial component depending on the sign of offset.

To prepare the input for the prediction algorithm, according to the relationship between the input and raw data, which are correlated to the mode of waves in receiver field, are required to multiply the synthetic gather. Therefore, before weighted multiplication, data has to be decomposed into P- and SV-wave components. First of all, after muting the direct waves, a cosine taper window is performed on the data for avoiding the affects of the Fourier transform due to the limited aperture. Then, data is decomposed into P- and SV-wave mode by applying Helmholtz's theorem, and separated components for P- and
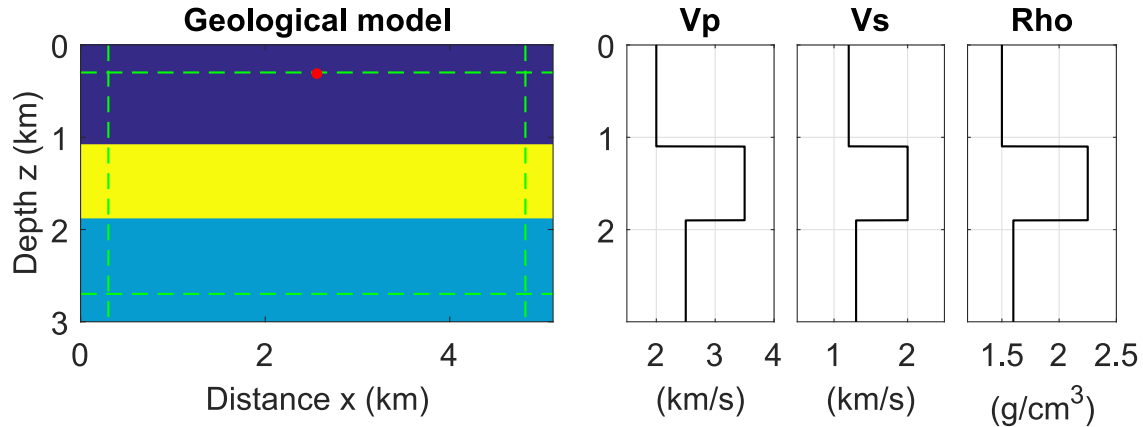
FIG. 2. Geological model and model parameters. The left panel shows a three layers geological model, the right panels indicate model parameters for P-, S-wave velocities, and density. From top to bottom, $v_p = [2.0, 3.5, 2.5]$ in km/s, $v_s = [1.2, 2.0, 1.3]$ in km/s, $\rho = [1.5, 2.25, 1.6]$ in g/cm^3.
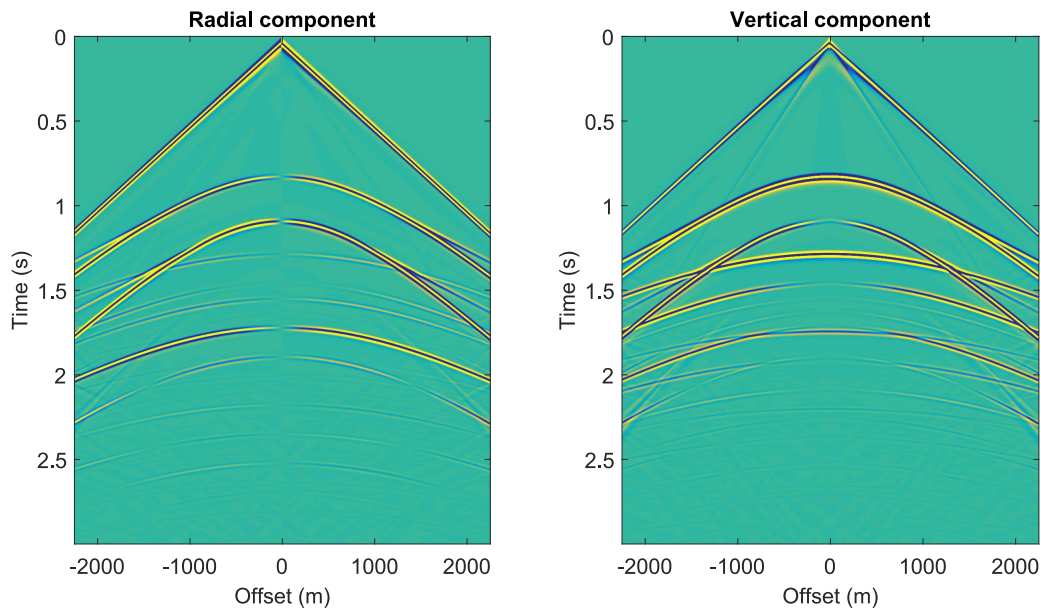

FIG. 3. A single shot gather. Left panel is the radial component, right panel is the vertical component.

S-waves are shown in Figure 4. Again, the polarity is symmetric over zero-offset in decomposed P-wave component, and is reversed over zero-offset in decomposed SV-wave component. The annotation and corresponded events of symbols (Figure 4) are shown in Table 1. There are four types of primary events both in decomposed P- and S-wave modes, delineated in first five rows in Table 1.

Here, Pr denotes 'primary' events, and IM represents the 'internal multiple'. The superscript delineates the wave mode in receiver wavefield. For primary event (Pr), the first number in subscripts is the related reflector number; the second number in subscript represents the number of S-wave raypath occurred in the current event (for P-wave mode, it equals to NO. S-wave raypath plus one; for S-wave mode, it equals to NO. S-wave raypath directly). Therefore, Pr_{22}^{P} denotes the primary in P-wave mode reflected by the second
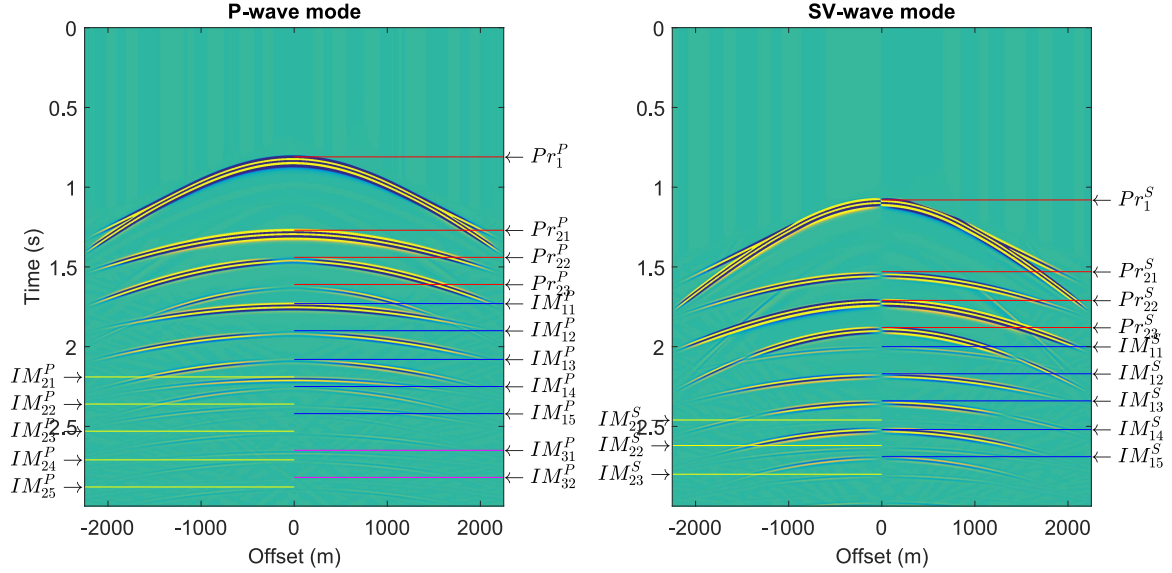
FIG. 4. Decomposed P- and SV-wave components of data in Figure 3.

reflector including two events: $\grave{P}\grave{P}\acute{S}\acute{P}$ & $\grave{P}\grave{S}\acute{P}\acute{P}$, which involve one S-wave raypath and both of them are recorded at the same time (here, accents represent downgoing ($\grave{X}$) and upgoing ($\acute{X}$) waves, respectively).

For internal multiples (IM), the first number in subscript denotes the order of internal multiples. And the second number in subscript describes the number of S-wave raypath, same criteria as described for primary events. Such as, IM_{22}^{S} are all second order internal multiples in S-wave mode which includes two S-wave raypath, i.e., $\grave{P}\grave{P}\acute{P}\grave{P}\acute{P}\grave{P}\acute{S}\acute{S}$, $\grave{P}\grave{P}\acute{P}\grave{P}\acute{P}\grave{S}\acute{P}\acute{S}$, $\grave{P}\grave{P}\acute{P}\grave{P}\acute{S}\grave{P}\acute{P}\acute{S}$, $\grave{P}\grave{P}\acute{P}\grave{S}\acute{P}\grave{P}\acute{P}\acute{S}$, $\grave{P}\grave{P}\acute{S}\grave{P}\acute{P}\grave{P}\acute{P}\acute{S}$, $\grave{P}\grave{S}\acute{P}\grave{P}\acute{P}\grave{P}\acute{P}\acute{S}$.

Input preparation

Eq. (6) indicates that elastic internal multiples can be predicted by the weighted decomposed data itself in a certain combination way. To estimate internal multiples in P- and SV-wave modes (i.e., $b_3^{\acute{P}\grave{P}}$ and $b_3^{\acute{P}\grave{P}}$), three inputs are required, $b_1^{\acute{P}\grave{P}}$, $b_1^{\acute{S}\grave{P}}$, and $b_1^{\acute{P}\grave{S}}$. As discussed above, the weighted decomposed input can be obtained using $b_1^{ij}(k_g^i, \omega) = \mathrm{i}2\nu^j D^{ij}(k_g^i, \omega)$. Expand this relations into decomposed P- and SV-wave mode, for a P-wave source only (i.e., $j = P$), we have,

$$b_1^{\acute{P}\grave{P}} = \mathrm{i}2\nu^P D^{\acute{P}\grave{P}} \tag{7a}$$

$$b_1^{\acute{S}\grave{P}} = \mathrm{i}2\nu^P D^{\acute{S}\grave{P}} \tag{7b}$$

$$b_1^{\acute{P}\grave{S}} = \mathrm{i}2\nu^S D^{\acute{S}\grave{P}} \tag{7c}$$

In plane wave domain, the preparation of inputs (Eq.(7)) can be rewritten by replacing

the vertical wavenumber (ν) into the vertical slowness q,

$$b_1^{\acute{P}\grave{P}}(p,\omega) = \mathrm{i}2q^P D^{\acute{P}\grave{P}}(p,\omega) \tag{8a}$$

$$b_1^{\acute{S}\grave{P}}(p,\omega) = \mathrm{i}2q^P D^{\acute{S}\grave{P}}(p,\omega) \tag{8b}$$

$$b_1^{\acute{P}\grave{S}}(p,\omega) = \mathrm{i}2q^S D^{\acute{S}\grave{P}}(p,\omega) \tag{8c}$$

where, the vertical slowness, for P-wave mode, can be calculated as,

$$q^P = \sqrt{\frac{1}{\alpha^2} - p^2} \tag{9}$$

for S-wave mode,

$$q^S = \sqrt{\frac{1}{\beta^2} - p^2} \tag{10}$$

Label-P	Primaries in P-mode	Label-S	Primaries S-mode
Pr_1^P	$\grave{P}\acute{P}$	Pr_1^S	$\grave{P}\acute{S}$
Pr_{21}^P	$\grave{P}\grave{P}\acute{P}\acute{P}$	Pr_{21}^S	$\grave{P}\grave{P}\acute{P}\acute{S}$
Pr_{22}^P	$\grave{P}\grave{P}\acute{S}\acute{P}$ & $\grave{P}\grave{S}\acute{P}\acute{P}$	Pr_{22}^S	$\grave{P}\grave{P}\acute{S}\acute{S}$ & $\grave{P}\grave{S}\acute{P}\acute{S}$
Pr_{23}^P	$\grave{P}\grave{S}\acute{S}\acute{P}$	Pr_{23}^S	$\grave{P}\grave{S}\acute{S}\acute{S}$

Label-P	1st-order IMs in P-mode	Label-S	1st-order IMs in S-mode
IM_{11}^P	$\grave{P}\grave{P}\acute{P}\grave{P}\acute{P}\acute{P}$	IM_{11}^S	$\grave{P}\grave{P}\acute{P}\grave{P}\acute{P}\acute{S}$
IM_{12}^P	$\grave{P}\grave{P}\acute{P}\grave{P}\acute{S}\acute{P}$	IM_{12}^S	$\grave{P}\grave{P}\acute{P}\grave{P}\acute{S}\acute{S}$
IM_{13}^P	$\grave{P}\grave{P}\acute{P}\grave{S}\acute{S}\acute{P}$	IM_{13}^S	$\grave{P}\grave{P}\acute{P}\grave{S}\acute{S}\acute{S}$
IM_{14}^P	$\grave{P}\grave{P}\acute{S}\grave{S}\acute{S}\acute{P}$	IM_{14}^S	$\grave{P}\grave{P}\acute{S}\grave{S}\acute{S}\acute{S}$
IM_{15}^P	$\grave{P}\grave{S}\acute{S}\grave{S}\acute{S}\acute{P}$	IM_{15}^S	$\grave{P}\grave{S}\acute{S}\grave{S}\acute{S}\acute{S}$

Label-P	2nd-order IMs in P-mode	Label-S	2nd-order IMs in S-mode
IM_{21}^P	$\grave{P}\grave{P}\acute{P}\grave{P}\acute{P}\grave{P}\acute{P}\acute{P}$	IM_{21}^S	$\grave{P}\grave{P}\acute{P}\grave{P}\acute{P}\grave{P}\acute{P}\acute{S}$
IM_{22}^P	$\grave{P}\grave{P}\acute{P}\grave{P}\acute{P}\grave{P}\acute{S}\acute{P}$	IM_{22}^S	$\grave{P}\grave{P}\acute{P}\grave{P}\acute{P}\grave{P}\acute{S}\acute{S}$
IM_{23}^P	$\grave{P}\grave{P}\acute{P}\grave{P}\acute{P}\grave{S}\acute{S}\acute{P}$	IM_{23}^S	$\grave{P}\grave{P}\acute{P}\grave{P}\acute{P}\grave{S}\acute{S}\acute{S}$
IM_{24}^P	$\grave{P}\grave{P}\acute{P}\grave{P}\acute{S}\grave{S}\acute{S}\acute{P}$		
IM_{25}^P	$\grave{P}\grave{P}\acute{P}\grave{S}\acute{S}\grave{S}\acute{S}\acute{P}$		

Label-P	3rd-order IMs in P-mode
IM_{31}^P	$\grave{P}\grave{P}\acute{P}\grave{P}\acute{P}\grave{P}\acute{P}\grave{P}\acute{P}$
IM_{32}^P	$\grave{P}\grave{P}\acute{P}\grave{P}\acute{P}\grave{P}\acute{P}\grave{S}\acute{P}$

Table 1. The annotation of symbols in Figure 4. Here, Pr denotes primary events, IM denotes internal multiples. The superscript represent type of wave mode in received field. In the subscripts of primaries, the 1st number denotes related reflector, the 2nd number minus one equals number of S-wave path between the fist and last path, i.e., Pr_{22}^P represent all events reflected by the second reflector involving one S-wave path between the first and last path, which are $\grave{P}\grave{P}\acute{S}\acute{P}$ & $\grave{P}\grave{S}\acute{P}\acute{P}$. In the subscripts of internal multiples, the 1st number denote the order of internal multiples, the 2nd number also represents number of S-wave pathe between the first and last wave path.

Here, α and β represent the P- and S-wave velocity in the background medium.

Figure 5 shows the $\tau - p$ transformed data in decomposed P- and S-waves mode, and primaries, internal multiples are color indicated as illustrated in Figrue 4. The weighted inputs data for $b_1^{\acute{P}\grave{P}}$, $b_1^{\acute{S}\grave{P}}$, are delineated in left, middle, and right panel of Figure 6. Note that, the first occurred events in $b_1^{\acute{P}\grave{P}}$, $b_1^{\acute{S}\grave{P}}$ are primaries $\grave{P}\acute{P}$, $\grave{P}\acute{S}$, and $\grave{S}\acute{P}$, which were reflected by the same reflector. Apparently, the events reflected at same depth were received at different traveltimes due to the velocity changes between P- and S-waves. It demonstrates
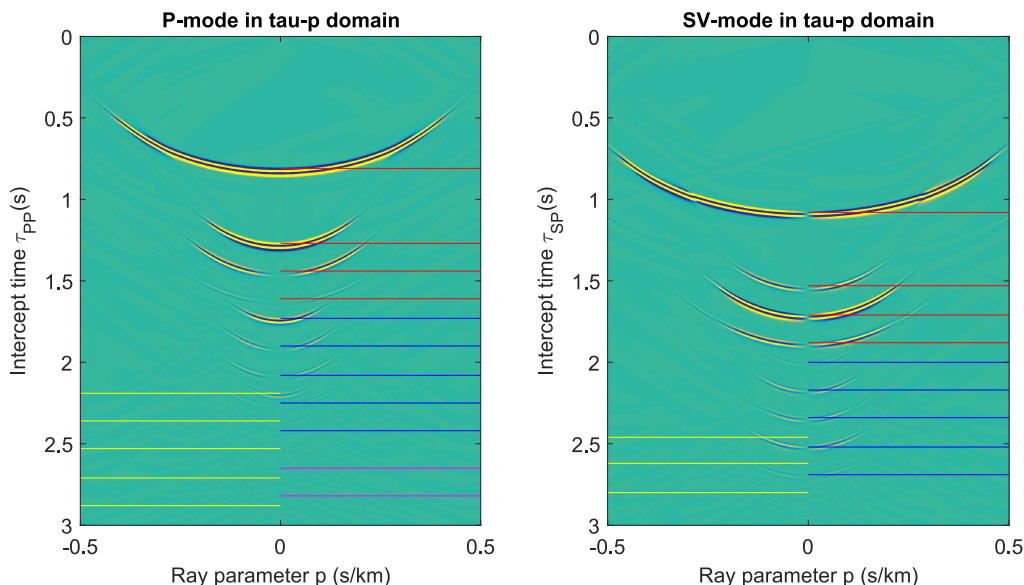
FIG. 5. Decomposed data in $\tau - p$ domain. The left panel: $\tau - p$ transformed decomposed P-wave component, the right panel: $\tau - p$ transformed decomposed SV-wave component.
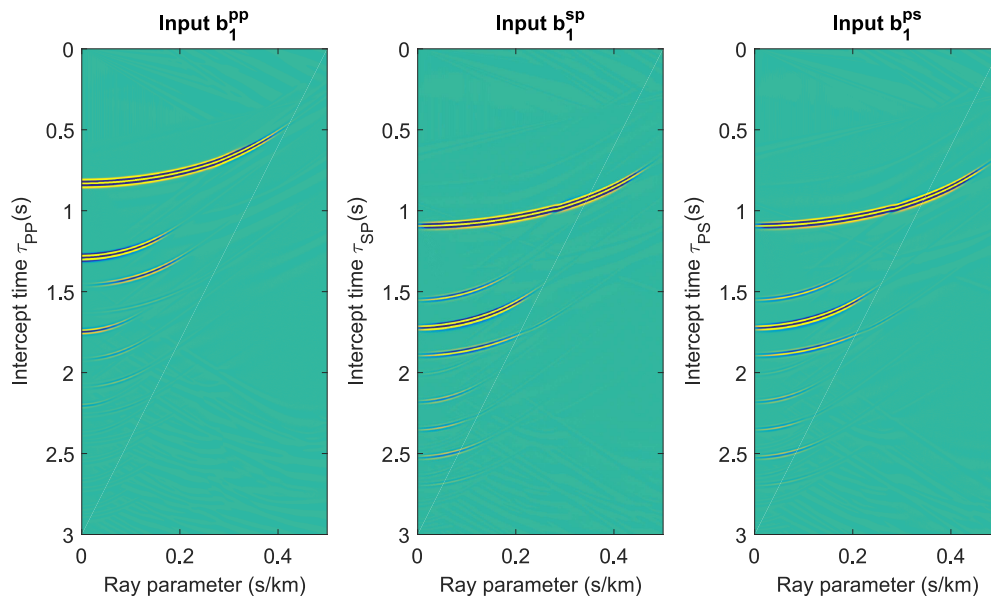

FIG. 6. Input data for elastic internal multiples prediction in plane wave domain, left panel - $b_1^{\acute{P}\grave{P}}$, middle panel - $b_1^{\acute{S}\grave{P}}$, and right panel - $b_1^{\acute{P}\grave{S}}$.

that the relationship between intercept time and pseudo-depth disobeys the monotonicity condition. In other words, the longer-shorter-longer combinations in intercept time cannot transfer to the lower-higher-lower relationship in pseudo-depth. Therefore, before transferring the algorithm into $\tau - p$ domain, the relationship between pseudo-depth (z) and intercept times (both τ_{PP} and τ_{PS}) has to be investigated.
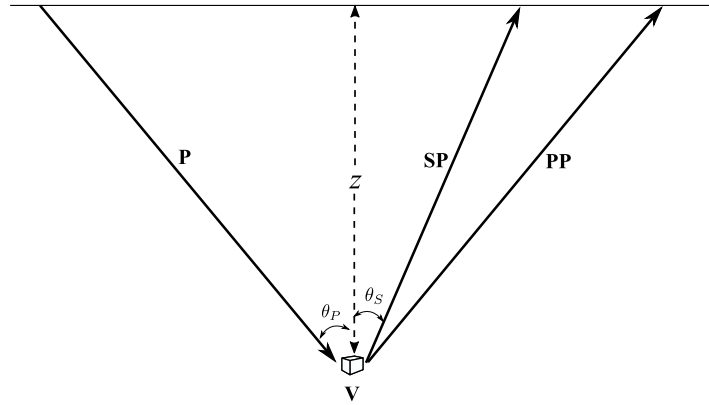
Integral limits and implementation in plane wave domain

FIG. 7. Raypaths of PP- and PS-waves propagating in a reference medium through one perturbation with P-wave source only.

Figure 7 describes raypaths of PP- and PS-waves propagating in a reference medium through one perturbation. The intercept times for PP- and PS-waves can be calculated as,

$$\tau_{PP} = 2\tau_P = \frac{2z \cos \theta_P}{\alpha} \tag{11a}$$

$$\tau_{SP} = \tau_P + \tau_S = z \left(\frac{\cos \theta_P}{\alpha} + \frac{\cos \theta_S}{\beta} \right) \tag{11b}$$

Combining Snell's law with Eq. (11), the relationship between τ_{PP} and τ_{SP} (or τ_{PS}) at the same pseudo-depth can be expressed as,

$$\tau_{SP} = \tau_{PS} = \frac{\alpha + \beta}{2\beta} \tau_{PP} \tag{12}$$

Eq. (12) indicates that, the comparison between two intercept times are related to its wave mode, and can be described as a function,

$$\Upsilon(\tau_2^{mn}|\tau_1^{nj}) = \begin{cases} \tau_2^{mn}, & j = m; \\ \frac{\alpha+\beta}{2\beta}\tau_2^{mn}, & j = S \ \& \ m = P; \\ \frac{2\beta}{\alpha+\beta}\tau_2^{mn}, & j = P \ \& \ m = S; \end{cases} \tag{13}$$

Here, $\Upsilon(\tau_2^{mn}|\tau_1^{nj})$ has the same identity as $\Upsilon(\tau_2^{mn}|\tau_1^{im})$ by placing j with i. Consider the transformation in Eq. (13), if relationship of two events in pseudo-depth is $z_2 > z_1$, the

corresponded intercept times between those two events can be written as $\Upsilon(\tau_2^{mn}|\tau_1^{nj}) > \tau_1^{nj}$, and vice versa. And Eq. (4) can be rewritten in the $\tau - p$ domain,

$$
b_3^{ij}(p_g, \omega) = -\int_{-\infty}^{+\infty} d\tau_1^{im} e^{i\omega\tau_1^{im}} b_1^{im}(p_g, \tau_1^{im}) \int_{-\infty}^{\Upsilon(\tau_1^{im}|\tau_2^{mn})-\epsilon} d\tau_2^{mn} e^{-i\omega\tau_2^{mn}} b_1^{mn}(p_g, \tau_2^{mn})
$$
$$
\times \int_{\Upsilon(\tau_2^{mn}|\tau_3^{nj})+\epsilon}^{+\infty} d\tau_3^{nj} e^{i\omega\tau_3^{nj}} b_1^{nj}(p_g, \tau_3^{nj})
$$

(14)

Considering the identity,

$$
\int_{-\infty}^{+\infty} dt' f(t') \int_{-\infty}^{t'-\epsilon_1} dt'' g(t'') = \int_{-\infty}^{+\infty} dt'' g(t'') \int_{t''+\epsilon_1}^{+\infty} dt' f(t')
$$
(15)

The plane wave domain prediction algorithm (Eq. 14) can be rewritten as,

$$
b_3^{ij}(p_g, \omega) = -\int_{-\infty}^{+\infty} d\tau_2^{mn} e^{-i\omega\tau_2^{mn}} b_1^{mn}(p_g, \tau_2^{mn}) \int_{\Upsilon(\tau_2^{mn}|\tau_3^{nj})+\epsilon}^{+\infty} d\tau_3^{nj} e^{i\omega\tau_3^{nj}} b_1^{nj}(p_g, \tau_3^{nj})
$$
$$
\times \int_{\Upsilon(\tau_2^{mn}|\tau_1^{im})+\epsilon}^{+\infty} d\tau_1^{im} e^{i\omega\tau_1^{im}} b_1^{im}(p_g, \tau_1^{im})
$$

(16)

However, Eq. (6) demonstrates that internal prediction, both for $b_3^{\acute{P}\grave{P}}$ and for $b_3^{\acute{S}\grave{P}}$, can be contributed by different combinations. Therefore, the rest combinations can be considered as the compensation to the first combination term. Which means, a more restricted limits applied in the rest combinations could prevent the suspicious events occurred in the final estimation. In sense of that, we adjust the limit relation function $\Upsilon(\tau_2^{mn}|\tau_1^{nj})$ into,

$$
\Gamma(\tau_2^{mn}|\tau_1^{nj}) = \begin{cases} \tau_2^{mn}, & j = m \; or \; j = P \;\&\; m = S; \\ \frac{\alpha+\beta}{2\beta}\tau_2^{mn}, & j = S \;\&\; m = P; \end{cases}
$$
(17)

Replacing the $\Upsilon(\tau_2^{mn}|\tau_1^{nj})$ by $\Gamma(\tau_2^{mn}|\tau_1^{nj})$ in Eq. (16), and considering the weighted decomposed P- and S-wave components in $\tau - p$ domain as the inputs (shown in Figure 6), we implement the elastic internal multiples prediction occurred in dataset shown in Figure 4.

The predicted elastic internal multiples are settled in decomposed P- and S-wave components, shown in Figure 8, respectively. Same color stratagem and symbols, as illustrated in Figure 4 and in Table 1, are labelled and indicated for primary and internal multiple events at zero-offset times. Compare the recorded seismic data in Figure 4 and the predicted multiples events in Figure 8, one can conclude that the primary events are well suppressed in the estimation, either in P-wave components or in S-wave components. Beyond that, all internal multiples occurred in recorded data are well estimated at its exactly traveltime. And no suspicious event and noise are generated in the prediction of internal multiples, which examines the elastic internal multiples prediction algorithm based on inverse scattering series we proposed in our companion paper (Sun and Innanen, 2016d).

Figure 9 and Figure 10 delineate the details of contribution by applying different combinations in Eq. (6). As we discussed above, the first term in Eq. (6) (both a and b) predicted
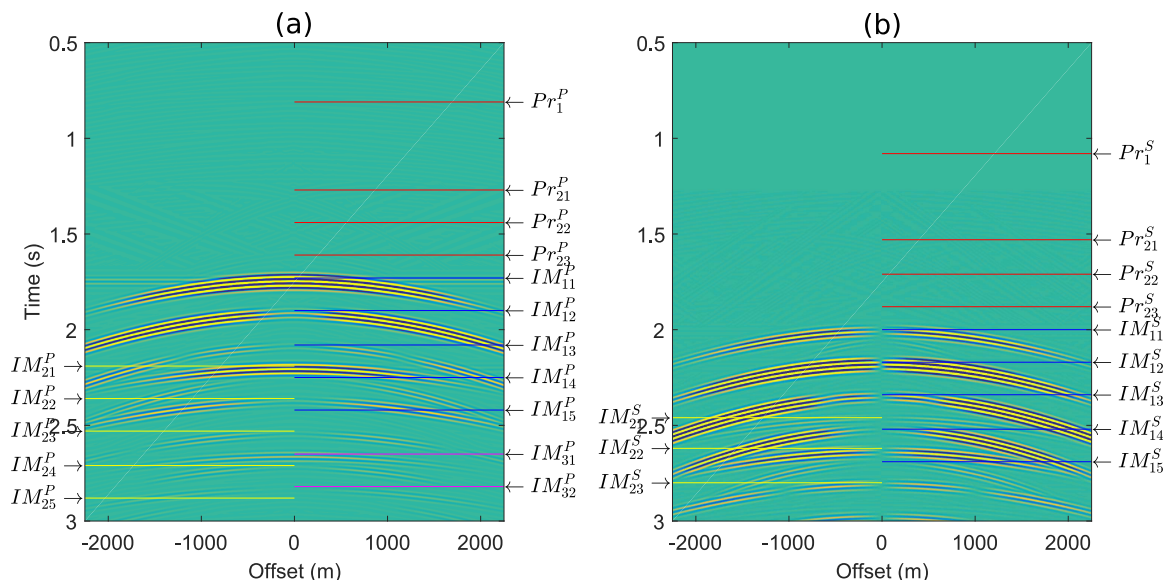
FIG. 8. Predicted elastic internal multiples occurred in Figure 4. (a) predicted elastic internal multiples in decomposed P-wave component, corresponded to data shown in left panel of Figure 4; (b) predicted elastic internal multiples in decomposed SV-wave component related to data shown in right panel of Figure 4.

the most of internal multiples occurred in seismic record data, but there are also some of them missing, such as IM_{13}^{P} and IM_{15}^{P} in P-wave component, and IM_{15}^{S} in S-wave component. Nevertheless, the rest combinable terms provide more information of those missed multiple events which, to a certain extent, compensate the shortcomings of the prediction by using first term only.

Above all, the elastic internal multiples prediction using inverse scattering series we proposed in a companion paper (Sun and Innanen, 2016d) can well handle the multiple prediction or elimination process, and the implementation details are discussed in this paper. The algorithm can be implemented in several variant domains, however, we recommend performing it in the plane wave domain as the discussion and investigation presented in an another companion paper (Sun and Innanen, 2016c).

CONCLUSIONS

Elastic internal multiples attenuation becomes to be a high priority problem to be solved in seismic data processing as the special significance of unconventional plays increasing rapidly, where the sophisticated quantitative interpretation is required. However, the existed internal multiple prediction algorithm, either needs extensive knowledge of subsurface or is not appropriate for an elastic medium. In our companion paper, we proposed the elastic internal multiple prediction algorithm based on inverse scattering series.

Following that, using a simple three-layer mode, we discussed how to prepare the input data for the prediction and showed how to implemented prediction in variant domains by recovering the monotonicity relationship between pseudo-depth and intercept time of P- and S-waves. Finally, the elastic internal multiples occurred in a three layers model were well estimated with precise traveltimes using the elastic ISS-IMP algorithm we proposed.
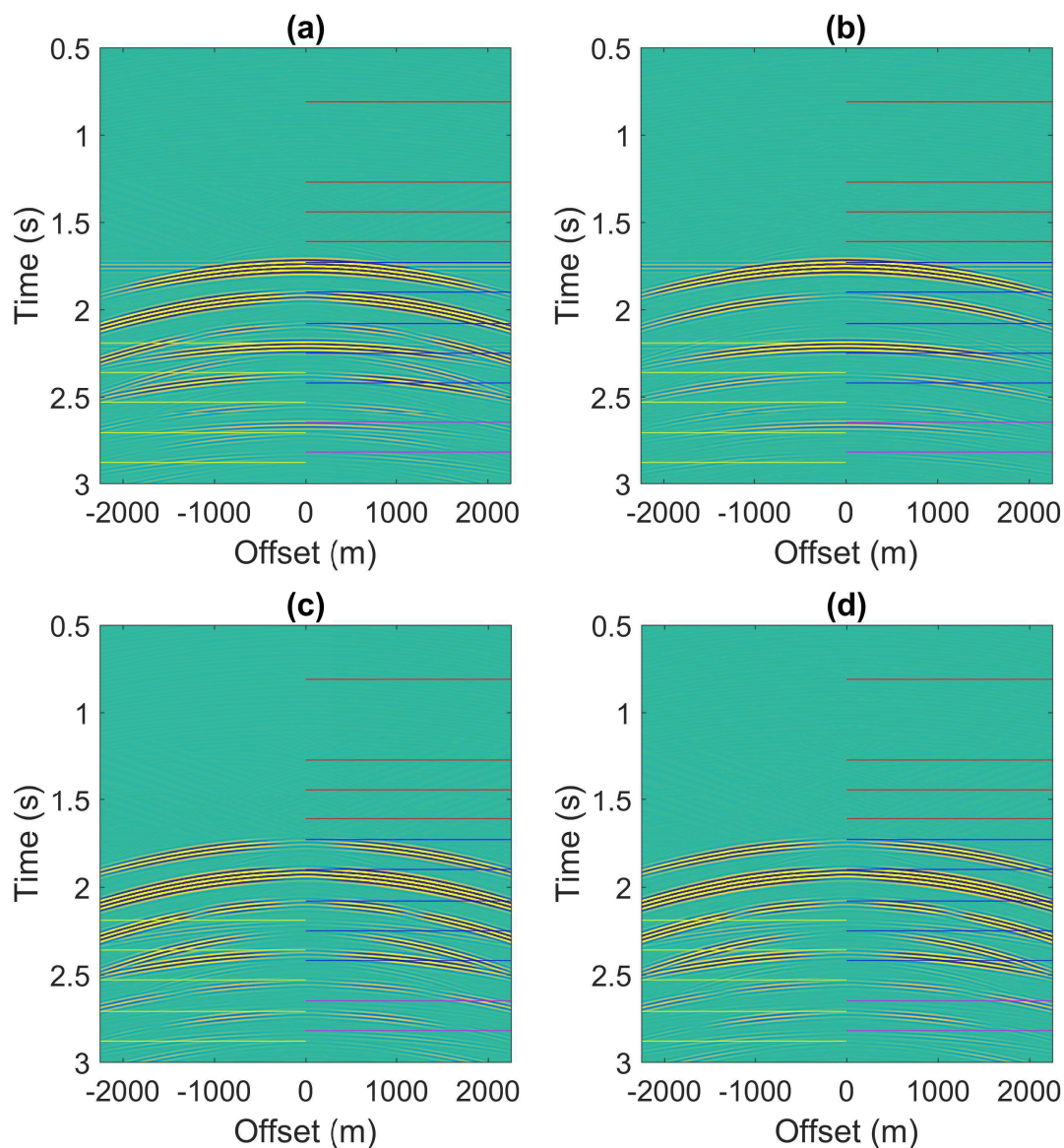
FIG. 9. Predicted elastic internal multiples in P-wave mode. (a) predicted elastic internal multiples in decomposed P-wave component, corresponded to data shown in left panel of Figure 4; (b) Elastic internal multiples prediction in P-wave mode using $\Theta_1(b_1^{\acute{P}\grave{P}})\Theta_2(b_1^{\acute{P}\grave{P}})\Theta_3(b_1^{\acute{P}\grave{P}})$, (c) Elastic internal multiples prediction in P-wave mode using $\Theta_1(b_1^{\acute{P}\grave{S}})\Theta_2(b_1^{\acute{S}\grave{P}})\Theta_3(b_1^{\acute{P}\grave{P}})$,(d) Elastic internal multiples prediction in P-wave mode using $\Theta_1(b_1^{\acute{P}\grave{P}})\Theta_2(b_1^{\acute{P}\grave{S}})\Theta_3(b_1^{\acute{P}\grave{P}})$.

The primary and suspicious events are refrained on high level. Further analysis of contributions from different combination terms are also investigated. Depending on investigation and predicted results, we can conclude that the elastic internal multiples prediction algorithm can be considered as an essential and potential technique for multiple elimination process, especially for complex land data.
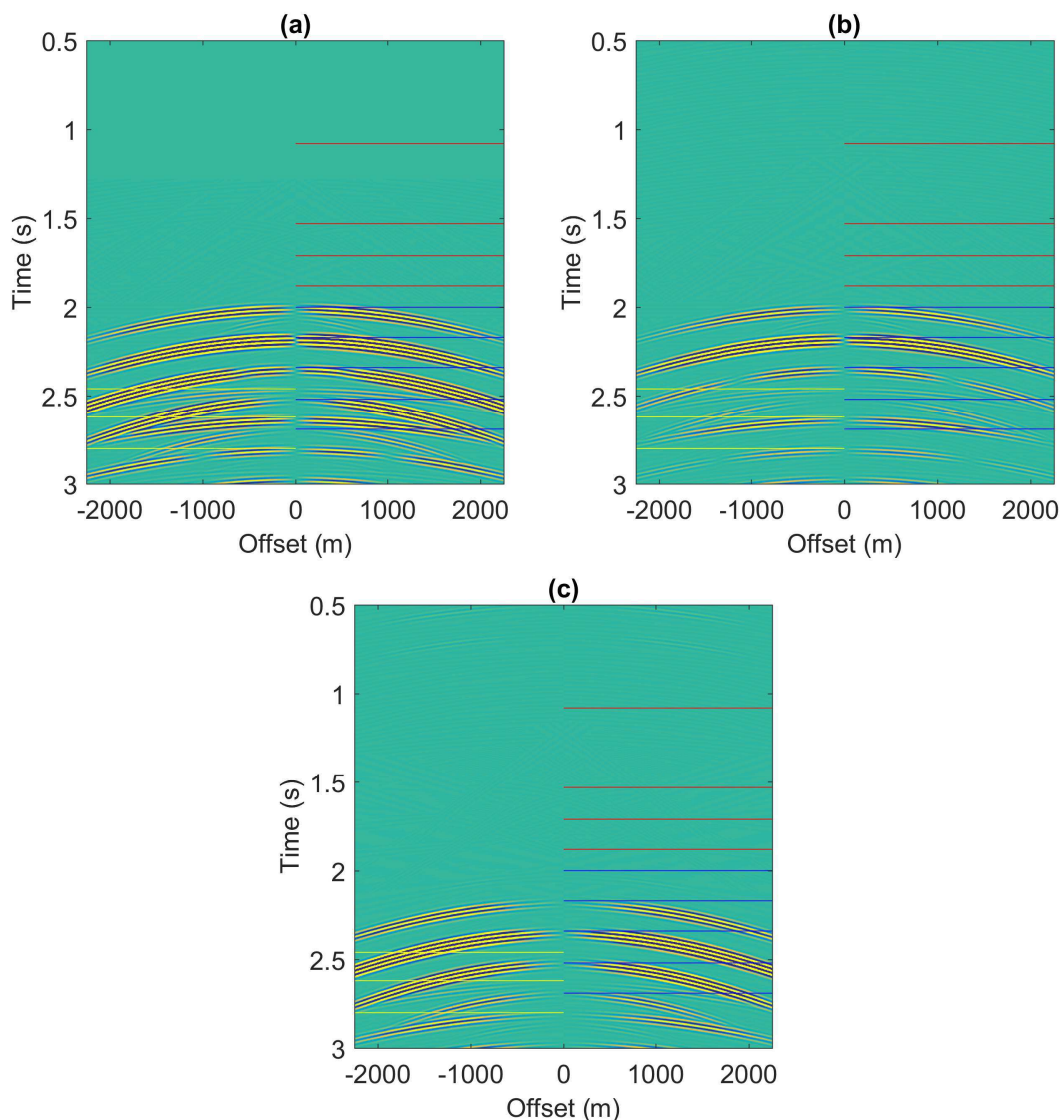
FIG. 10. Predicted elastic internal multiples in S-wave mode. (a) predicted elastic internal multiples in decomposed S-wave component, corresponded to data shown in right panel of Figure 4; (b) Elastic internal multiples prediction in S-wave mode using $\Theta_1(b_1^{\acute{S}\grave{P}})\Theta_2(b_1^{\acute{P}\grave{P}})\Theta_3(b_1^{\acute{P}\grave{P}})$, (c) Elastic internal multiples prediction in S-wave mode using $\Theta_1(b_1^{\acute{S}\grave{P}})\Theta_2(b_1^{\acute{P}\grave{S}})\Theta_3(b_1^{\acute{P}\grave{P}})$.

ACKNOWLEDGEMENTS

REFERENCES

Araujo, F. V., Weglein, A. B., Carvalho, P. M., and Stolt, R., 1994, Inverse scattering series for multiple attenuation: An example with surface and internal multiples, Tech. rep., Society of Exploration Geophysicists, Tulsa, OK (United States).

Berkhout, A., 2006, Seismic processing in the inverse data space: Geophysics, **71**, No. 4, A29–A33.

Berkhout, A., and Verschuur, D., 2005, Removal of internal multiples with the common-focus-point (cfp) approach: Part 1–explanation of the theory: Geophysics, **70**, No. 3, V45–V60.

Hernandez, M., and Innanen, K. A. H., 2014, Identifying internal multiples using 1d prediction: Physical modelling and land data examples: Canadian journal of exploration geophysics, **39**, No. 1, 37–47.

Innanen, K. A. H., 2016a, Time and offset domain internal multiple prediction with nonstationary parameters, *in* SEG Technical Program Expanded Abstracts 2016, Society of Exploration Geophysicists, 4518–4523.

Innanen, K. A. H., 2016b, Time domain internal multiple prediction: CSEG Geoconvention.

Kelamis, P., Erickson, K., Burnstad, R., Clark, R., and Verschuur, D., 2002a, Data-driven internal multiple attenuationâĂŤapplications and issues on land data: Soc. of Expl. Geophys, 2035–2038.

Kelamis, P. G., Erickson, K. E., Verschuur, D. J., and Berkhout, A., 2002b, Velocity-independent redatuming: A new approach to the near-surface problem in land seismic data processing: The Leading Edge, **21**, No. 8, 730–735.

Liu, F., Sen, M. K., and Stoffa, P. L., 2000, Dip selective 2-d multiple attenuation in the plane-wave domain: Geophysics, **65**, No. 1, 264–274.

Luo, Y., Zhu, W., Kelamis, P. G. et al., 2007, Internal multiple reduction in inverse-data domain: SEG Expanded Abstracts. San Antonio:[sn], 125–129.

Ma, J., Sen, M. K., and Chen, X., 2009, Free-surface multiple attenuation using inverse data processing in the coupled plane-wave domain: Geophysics, **74**, No. 4, V75–V81.

Matson, K. H., 1997, An inverse scattering series method for attenuating elastic multiples from multicomponent land and ocean bottom seismic data: Ph.D. thesis, University of British Columbia.

Pan, P., 2015, 1.5 d internal multiple prediction: an application on synthetic data, physical modelling data and land data synthetics: M.Sc. thesis, University of Calgary.

Pan, P., and Innanen, K. A. H., 2015, 1.5d internal multiple prediction on physical modeling data: CSEG Geoconvention.

Pan, P., Innanen, K. A. H. et al., 2014, Numerical analysis of 1.5 d internal multiple prediction, *in* 2014 SEG Annual Meeting, Society of Exploration Geophysicists.

Sun, J., and Innanen, K., 2016a, Interbed multiple prediction on land: which technology, and which domain?: CSEG Recorder, **41**, No. 10, 24–29.

Sun, J., and Innanen, K. A. H., 2014, 1.5d internal multiple prediction in the plane wave domain: CREWES Research Report, **26**, 1–11.

Sun, J., and Innanen, K. A. H., 2015, 1.5 d internal multiple prediction in the plane wave domain: CSEG Geoconvention.

Sun, J., and Innanen, K. A. H., 2016b, Extension of internal multiple prediction: 1.5 d to 2d in double plane wave domain: CSEG Geoconvention.

Sun, J., and Innanen, K. A. H., 2016c, Literature review and discussions of inverse scattering series on internal multiple prediction: CREWES Research Report, **28**, 1–24.

Sun, J., and Innanen, K. A. H., 2016d, Theoretical framework of elastic internal multiples prediction based on inverse scattering series: CREWES Research Report, **28**, 1–21.

Taner, M., 1980, Long period sea-floor multiples and their suppression: Geophysical Prospecting, **28**, No. 1, 30–48.

Verschuur, D. J., 1991, Surface-related multiple elimination, an inversion approach: Ph.D. thesis, Technische Univ., Delft (Netherlands).

Weglein, A. B., Araújo, F. V., Carvalho, P. M., Stolt, R. H., Matson, K. H., Coates, R. T., Corrigan, D., Foster, D. J., Shaw, S. A., and Zhang, H., 2003, Inverse scattering series and seismic exploration: Inverse problems, **19**, No. 6, R27.

Weglein, A. B., Gasparotto, F. A., Carvalho, P. M., and Stolt, R. H., 1997, An inverse-scattering series method for attenuating multiples in seismic reflection data: Geophysics, **62**, No. 6, 1975–1989.

Zou, Y., and Weglein, A. B., 2015, An internal-multiple elimination algorithm for all first-order internal multiples for a 1d earth, *in* 2015 SEG Annual Meeting, Society of Exploration Geophysicists.